Bloch walls in a nickel single crystal

J. Peters and W. Treimer
Technische Fachhochschule Berlin (University of Applied Sciences), Luxemburger Strasse 10, D-13353 Berlin, Germany
and Hahn-Meitner-Institut Berlin, Glienicker Strasse 100, D-14109 Berlin, Germany
(Received 28 November 2000; published 13 November 2001)

We present a consistent theory for the dependence of the magnetic structure in bulk samples on external static magnetic fields and corresponding experimental results. We applied the theory of micromagnetism to this crystal and calculated the Bloch wall thickness as a function of external magnetic fields. The theoretical results agree well with the experimental data, so that the Bloch wall thickness of a ⟨110⟩ 71° nickel single crystal was definitely determined with some hundred of nanometer.

DOI: 10.1103/PhysRevB.64.214415 PACS number(s): 75.60.Ch, 75.50.Cc, 28.20.Cz

I. INTRODUCTION

Ferromagnetic (crystalline) materials such as iron, nickel, and cobalt show in small regions (Weiss domains) a spontaneous magnetization, whereas these domains are randomly distributed over the whole crystal. Applying a small external magnetic field to the sample the randomly orientated domains tend to align towards each other to minimize the total energy. To reach this minimum state, different competing energies force the system to build up magnetic domains, e.g., to reduce stray field energy and to bring the atomic spins into ''easy'' directions of magnetization.[1–4]

The study of ferromagnetic domains is of principle interest, especially the interaction between external macroscopic forces (pressure, tension, torsion) and the magnetism of a sample. Obviously there is no common known universal quantum theory of ferromagnetism which describes sufficiently well and in general terms all effects of micromagnetism and macromagnetism. The theory of micromagnetism, however, is accurate enough to reproduce the behavior of magnetic materials, their magnetism, and the magnetic structure inside of a ferromagnetic sample. It enables the inclusion of a number of different energy contributions and the calculation of the magnetic structure of a sample. For nickel crystals, e.g., there exist only a few theoretical studies and experiments on magnetic domains in bulk samples,[5,6] mainly due to the lack of suitable samples and due to the experimental difficulties. They are manifold: On the one hand there is a radiation which mainly interacts with the bulk magnetism of the sample and, on the other hand, one can hardly deduce the interior magnetic structure from surface observations as with Bitter pattern technique or Kerr effect microscopy. Especially the latter method has been perfectly applied to image surface structures.[7] However, there remains the uncertainty of the inner magnetic structure in the bulk of a sample. The past surface observations of nickel crystals were performed very extensively by Schwink and Spreen,[4] who developed some ideas of the inner domain structure in ⟨100⟩ and ⟨110⟩ nickel single crystals. These authors and other groups[5,6,8] carried out experimental works on the Bloch wall structures in the last years for iron and nickel and reported different values for the Bloch walls' thicknesses.

The best radiation to investigate magnetic structures in the bulk of samples are neutrons due to their electric neutrality and their magnetic moment μ_N which interacts with magnetic fields. Therefore, the spin dependent refraction of unpolarized neutrons by these Bloch walls is an already well established and reliable method to investigate their thickness as a sensitive parameter if the system reaches its state of minimum energy. The angles of refraction are extremely small (sec of arc), so they can only be observed with a high resolution double crystal diffractometer (see below). The integrated intensities of the refracted neutrons are proportional to the thickness of the Bloch wall and can be determined quite accurately.

In the second part we present our theoretical results on this subject. In the third part the experimental setup and the measurements are given. In the fourth part we discuss some applications and give the results.

II. THEORY OF MICROMAGNETISM APPLIED TO A ⟨110⟩ 71° NICKEL SINGLE CRYSTAL

The theory of micromagnetism (for details see Refs. 7, 9–11) is a phenomenological theory which describes the behavior of ferromagnetic materials on an intermediate scale between atomic lattice sites (nanometer) and domains of some hundred micrometer. This scale is small enough to reveal details of transition regions between domains and yet large enough to permit the use of a continuous magnetization vector **I**. For a constant temperature and far off from the Curie point I_S, the magnitude of **I**, can be assumed to be constant. **I** is defined as

$$\mathbf{I}=I_s\boldsymbol{\alpha}(\mathbf{r}), \quad \sum_{i=1}^{3}\alpha_i^2=1, \tag{1}$$

where the α_i's are the direction cosines of the magnetization. To calculate the minimum of the total (free) energy of the system and furthermore the Bloch wall thickness one has to solve the variation problem

$$\delta_\alpha\{\int(e_A+e_K+e_{H_a})dV+E_s+E_{\mathrm{ms}}\}=0, \tag{2}$$

with the constraint

$$\sum_{i=1}^{3}\alpha_i^2=1.$$

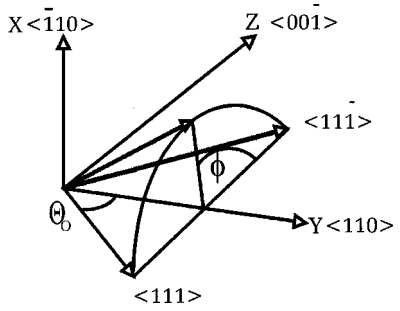

FIG. 1. Crystal directions of the ⟨110⟩ nickel crystal (see also Fig. 2).

In Eq. (2) the following energy density contributions are taken into account: The exchange energy density e_A, the crystalline energy density for a cubic crystal e_K, and the magnetostatic energy density e_{H_a}, where $\mathbf{H}_a$ is the external magnetic field. The other energy contributions, i.e., the stray field energy E_s and the magnetostrictive energy E_{ms}, contain in general the contribution of the whole sample, therefore one has to integrate over the total volume. For special problems (for instance, one-dimensional plane Bloch walls as in our case) the stray field energy and the magnetostrictive energy can also be written as local energy densities e_S and e_{ms}.[11]

To apply the theory of micromagnetism we consider the well known system of a ⟨110⟩ 71° nickel single crystal. This choice does not restrict our calculations to this system but the results can directly be proved by experimental data. Nickel has a body-centered cubic crystal structure and without the influence of external forces or fields the ⟨111⟩ directions of easy magnetization correspond to a minimum crystalline energy e_K. Depending on the orientation of the crystal axis there are different possibilities for the angles between the directions of easy magnetization. The ⟨110⟩-direction of the crystal axis corresponds in our case to the y-axis and the angle $\theta_0 \approx 35{,}3°$ is the angle between the easy direction and the crystal axis. This type of Bloch wall is abbreviated as ⟨110⟩ 71° Bloch wall, where the 71° stands for $2\theta_0$ (see Fig. 1). The energy density contributions can be calculated according to Hubert[11] or Hubert and Schäfer.[7]

The magnetization vector **I** rotates within the Bloch wall keeping the angle θ_0 nearly constant by altering ϕ only and avoiding stray fields by taking this path. This kind of rotation is realized in most ferromagnetic materials, because it leads to less total energy. To determine the constant angle θ_0 and the angles ϕ_a and ϕ_e corresponding to the two alternating directions of the magnetization in the adjacent domains, one has to solve a boundary condition problem by minimizing the energy density contributions in the domains. Whereas the values for ϕ_a and ϕ_e remain almost unchanged under different external conditions and stay equal to $\phi_a = 0°$ and $\phi_e = 180°$, the value for θ_0 strongly depends on the external conditions, i.e., fundamentally on the magnitude of the external magnetic field H_a.

In the presence of such an additional external field the actual constant angle θ_0 does not necessarily correspond to the energy density minimum. The path of **I** from one easy direction to the other may slightly differ from the path with θ kept fixed and equal to θ_0. It is thus possible to find the value of the angle θ between the magnetization vector **I** and the crystal axis corresponding to the actual minimum by expanding the variational equation (2) around the angle θ_0 and by solving Euler's equation as proposed by Döring.[12] These corrections lead to small contributions, even for the stray field energy density. With this treatment one can calculate the total energy E_{tot}, which is necessary to describe the rotation of **I**, and the Bloch wall thickness.

For the special case of the ⟨110⟩ 71° nickel single crystal one calculates first with the zero order of the expansion (e.g., $\theta \approx \theta_0$) the energy contained in the Bloch wall per surface unit (in J/m^2) to be

$$E_0 = 2\sqrt{A}\sin\theta_0 \int_{\phi_a}^{\phi_e} [(e_k(\theta_0,\phi_0) - e_K^{\infty}) + e_{\mathrm{ms}}(\theta_0,\phi_0)]^{1/2} d\phi_0, \tag{3}$$

where A is the exchange constant and $\phi_0(y)$ the zero order approximation for the path $\phi(y)$. The Bloch wall thickness then reads

$$W_L^0 = \frac{\pi\sqrt{A}\sin\theta_0}{\sqrt{[e_K(\theta_0,\phi_W) - e_K^{\infty}] + e_{\mathrm{ms}}(\theta_0,\phi_W)}}, \tag{4}$$

where ϕ_W is the point of inflection of the function $\phi_0(y)$, which is here very close to $\pi/2$. Equations (3) and (4) are identical with the expressions proposed by Hubert.[11] Following further Döring[12] it is possible to use a higher order in the expansion around θ_0 with the help of the small expansion parameter λ defined below. Then one obtains the energy of the Bloch wall per unit of the surface

$$E_1 = \lambda \frac{\sqrt{A}}{K_1}\sin\theta_0 \left\{ \int_{\phi_a}^{\phi_e} \frac{\left(\frac{1}{2}\left(\frac{\partial e_K}{\partial u}\right)_{u=0} - \frac{\cos\theta_0}{\sin^2\theta_0}[e_K(\theta_0,\phi_0) - e_K^{\infty} + e_{\mathrm{ms}}(\theta_0,\phi_0)] \right)^2}{\sqrt{[e_K(\theta_0,\phi_0) - e_K^{\infty}] + e_{\mathrm{ms}}(\theta_0,\phi_0)}} d\phi_0 \right\}$$

$$- \frac{2\sqrt{A}\lambda}{\tan\theta_0} \left\{ \int_{\phi_a}^{\phi_e} \left(h + \frac{1}{2K_1}\left(\frac{\partial e_{\mathrm{ms}}}{\partial u}\right)_{u=0} \right) \sqrt{[e_K(\theta_0,\phi_0) - e_K^{\infty}] + e_{\mathrm{ms}}(\theta_0,\phi_0)}\, d\phi_0 \right\}$$

$$+\frac{\sqrt{A}}{K_1}\lambda\sin\theta_0\left\{\int_{\phi_a}^{\phi_e}\left[\left(\frac{\partial e_{\mathrm{ms}}}{\partial u}\right)_{u=0}\left\{\frac{1}{2}\left(\frac{\partial e_K}{\partial u}\right)_{u=0}+hK_1+\frac{1}{4}\left(\frac{\partial e_{\mathrm{ms}}}{\partial u}\right)_{u=0}\right\}+K_1\left(\frac{\partial e_K}{\partial u}\right)_{u=0}h+K_1^2h^2\right]\right.$$

$$\left.\times\frac{d\phi_0}{\sqrt{[e_K(\theta_0,\phi_0)-e_K^{\infty}]+e_{\mathrm{ms}}(\theta_0,\phi_0)}}\right\}, \tag{5}$$

where K_1 is the crystalline energy constant. Furthermore we used the abbreviation $h=-H_aI_s/2K_1$, the parameter $\lambda=-K_1\mu_0/2\pi I_S^2$, where μ_0 is the magnetic field constant, and $u=\cos\theta-\cos\theta_0$. The Bloch wall thickness can be obtained by taking the first order of the expansion and replacing in Eq. (4) the constant angle θ_0 by the angle $\theta_W=\theta_1(\phi_W)$, where θ_1 designates the higher order term in the expansion of θ around the constant angle θ_0.

III. METHOD OF MEASUREMENT AND EXPERIMENTAL SETUP

A. Method

The interaction of neutrons with magnetic materials is described by the Hamiltonian operator $\hat{H}$ applied to the system under investigation:

$$\hat{H}=\frac{1}{2m}p^2+V(r)-\boldsymbol{\mu}\cdot\mathbf{B}, \tag{6}$$

where p is the momentum of the neutron, $V(r)$ the nuclear interaction potential, $\boldsymbol{\mu}$ the magnetic moment, and **B** the magnetic induction. The neutron experiences a constant interaction potential if it passes the magnetic material, therefore one can use the time independent Schrödinger equation to calculate its behavior in the system

$$\hat{H}\psi(r)=E\psi(r) \tag{7}$$

or

$$(\nabla^2+k_0^2)\psi(r)-\frac{2m}{\hbar^2}[V(r)+\boldsymbol{\mu}_n\cdot\boldsymbol{\sigma}\cdot\mathbf{B}]\psi(r)=0 \tag{8}$$

with $k_0=$ vacuum wave vector of the neutron $k_0=2\pi/\lambda$ and $\boldsymbol{\sigma}=$ Pauli spin matrices.

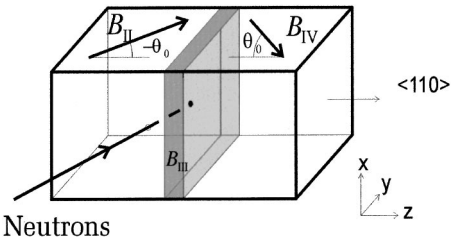

FIG. 2. The two adjacent magnetic domains B_{II} and B_{IV} are separated by a Bloch wall B_{III}, i.e., a region where the induction **B** rotates from B_{II} to B_{IV}. θ_0 means the angle between the induction **B** with respect to crystal axis (y direction in Fig. 1).

We use the spin dependent refraction of unpolarized neutrons by Bloch walls. Neutrons experience a potential jump if they enter a region of uniform magnetization **B**, depending on the spin states parallel or antiparallel with respect to **B**. The boundary conditions are the continuity of the wave function at the entrance point on the surface of the crystal (entering into the first domain, see Figs. 2 and 3). Due to the fact that the nuclear potential in the crystal is constant, only the magnetic potential jump has to be calculated if a neutron traverses the Bloch wall, i.e., if the neutron passes from one magnetic domain into the other. The Bloch wall itself separates two differently orientated **B**'s and is supposed to be ''thin'' in the sense that $\omega\geqslant\omega_L$, where ω equals the effective rotation frequency of **B** the neutron experiences if it passes the Bloch wall and ω_L is the Larmor frequency of the neutron. The solution of Eq. (8) for the total system yields the transmission probabilities of a neutron which (a) enters a magnetic domain in the crystal, (b) traverses a Bloch wall, (c) enters the adjacent domain, and (d) leaves the crystal at the exit surface (Fig. 2) (for a detailed description see Refs. 6, 8). The transmitted intensity depends on the wavelength of the neutron λ, the saturation magnetization of nickel B_s, the angle θ_0 (see above) and the thickness d of the Bloch wall. Vice versa, the Bloch wall thickness W_L can be determined by measuring the transmitted refracted intensity of neutrons. If the neutron passes a Bloch wall its wave vectors for spin parallel and spin antiparallel relative to **B** change their direction and so the flight direction. Therefore the neutrons with spin up and down have different directions if they exit the crystal, indicated by the angles α_+ and α_- (Fig. 3). These angles are of the order of sec of arc which only can be detected as satellites of a main peak with a high resolution double crystal diffractometer (DCD). The integrated intensities of these satellites for a given angle of incidence α and refraction angles α_+ and α_- are proportional to the transmission probabilities of neutrons which traverse a Bloch wall

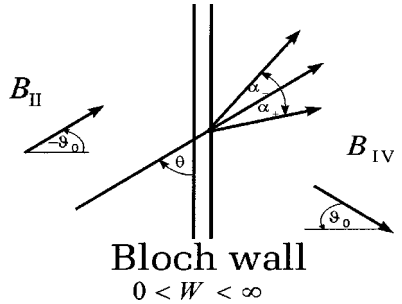

FIG. 3. Spin splitting due to (partial) refraction of unpolarized neutrons by a Bloch wall.

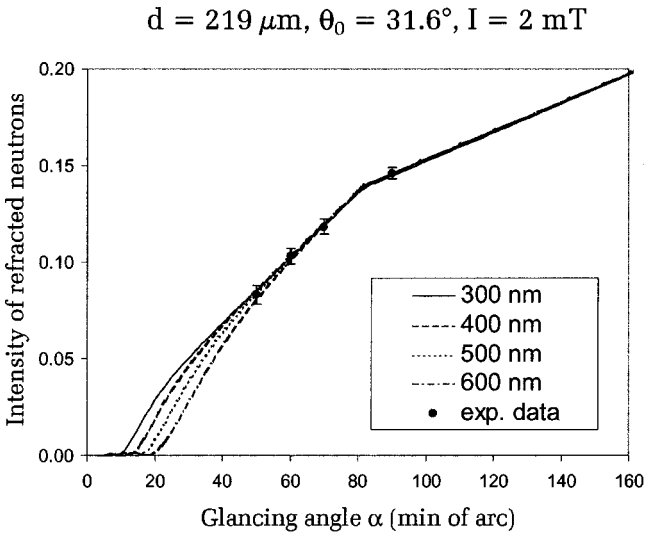

FIG. 4. Transmitted refracted intensity I_{refr} as a function of the glancing angle α for different Bloch wall thicknesses W_L. Note the behavior of the transmitted intensity for glancing angles larger than $90'$.

with the thickness W_L. Measuring different transmission probabilities for different angles of incidence α, one gets a curve representing the transmission curve for a certain Bloch wall thickness W_L.

Figure 4 shows an example for the transmitted intensity I_{refr} as a function of $W_L = 300\,\mathrm{nm}$ until $W_L = 600\,\mathrm{nm}$ for a calculated $\theta_0 = 31.6°$, a neutron wavelength $\lambda = 0.268\,\mathrm{nm}$ and domain width $b = 219\,\mu\mathrm{m}$. As can be seen, the fraction of the total refracted intensity decreases rapidly for small glancing angles. However, to distinguish different Bloch wall thicknesses one has to use glancing angles α between $30'$ $-90'$. For glancing angles $\alpha > 90'$ the transmission probability of neutrons becomes nearly independent of W_L. These facts show the problem of measuring W_L with a sufficient degree of accuracy allowing an uncertainty of only a few percent. The smaller the glancing angle is the smaller the refracted intensity becomes, which is already very low due to the use of a high resolution DCD.

B. Experimental setup

To measure the spin dependent refraction of unpolarized neutrons we used the high angular resolution DCD E8 of the Hahn-Meitner-Institut (Fig. 5). The DCD consists of a pair of perfect crystals (Si, (220) symmetric reflection): One crystal acting as monochromator (in the neutron guide), the other as analyzer crystal. The analyzer is placed in a polyethylene shielding to suppress background radiation and to keep the crystal at a constant temperature. The entrance and the exit windows are covered with thin Al sheets. The angular stepping resolution of the analyzer rotation stage is better than a 0.1 sec of arc, because it guarantees a smooth scanning of the rocking curve. The nickel sample was placed outside the concrete shielding between the two crystals (Fig. 5) on a special rotation stage. In front of the sample a soller collimator reduces the beam divergence down to 10 min of arc to

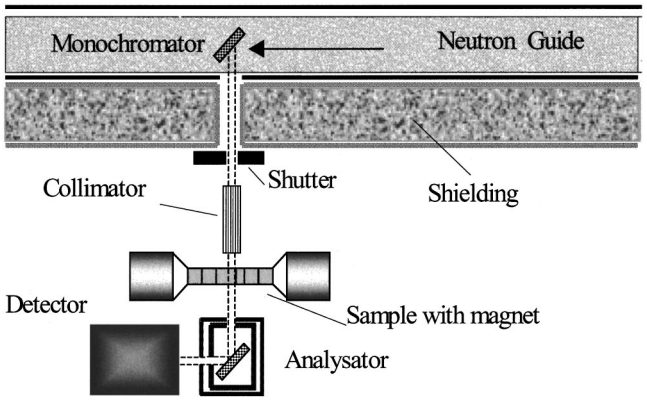

FIG. 5. The double crystal diffractometer (DCD) E8 at the BER II reactor at the Hahn–Meitner-Institute Berlin. Monochromator and analyzer are perfect Si crystals, (220) symmetrical reflection; mean wavelength $\lambda = 0.268(1)$ nm.

define the incident beam direction onto the Bloch wall within the desired accuracy and to avoid smearing effects that occurs as a result of a too large variation of the glancing angles (see Fig. 4).

To get an ordered and defined system of Bloch walls a small magnetic field ($2-7\,\mathrm{mT}$) was applied to the nickel sample yielding a nearly parallel orientation of the Bloch walls to each other. The parallel position of the Bloch walls relative to the incident neutron beam was found by rotating the Bloch walls around an axis perpendicular to the scattering plane whereas the analyzer crystal was kept in its maximum position of the rocking curve. If the Bloch walls are parallel to the neutron beam ($\alpha_{+,-} \sim 0$), no refraction occurs. If α increases (see Figs. 3, 4) the part of the neutron beam which hits the wall increases and more neutrons are refracted. Due to the deviation from the initial flight direction the neutrons are not reflected by the analyzer crystal. The measured intensity decreases. As the refraction angle $\alpha_{+,-}$ decreases with increasing α, both refracted peaks come closer to the main peak until they cannot be distinguished from each other. The reflected intensity increases with increasing α again until it reaches an intensity which is of a similar intensity of the parallel position of the Bloch walls to the neutron beam. In that case the angles of refraction $\alpha_{+,-}$ are too small to be distinguished from the incident position.

The parallel position of the Bloch wall with respect to the incident neutron beam is found by fitting a suitable function symmetric to the measured points around $\alpha \sim 0$. Then the angle of incidence α can be assumed with an accuracy better than 5 min of arc. The experiments are performed (a) by setting different static magnetic fields to the sample and (b) by setting different α and measuring the refracted intensity under these well-defined conditions.

IV. EXPERIMENTAL RESULTS

The nickel single crystal used for the investigations was produced by the MSG-Metallschmelz-GmbH and is described in detail in Ref. 8. It has a length of 76 mm in $\langle 110 \rangle$ (y direction), a width of 9,2 mm (z direction), and a height of

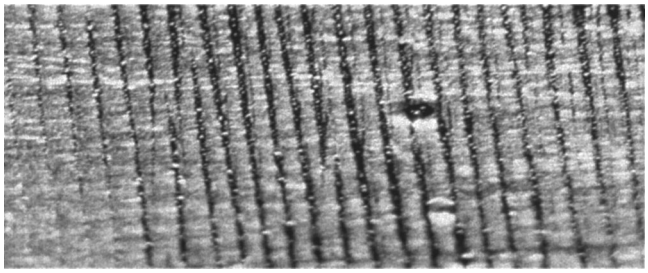

FIG. 6. Bloch walls and domains observed on the surface of a nickel single crystal by Bitter technique, displayed length is ~50 mm.

13,2 mm (x direction). We took experimental data for the magnetic constants from literature. The values for the magnetization of saturation I_s and the crystalline anisotropy constants K_1 and K_2 (at room temperature) are from Ref. 13: $I_s = 0{,}62$ T, $K_1 = -5700$ J/m^3, and $K_2 = -2300$ J/m^3. The value for K_1 is very similar to the one given in Ref. 14 and to the data in Ref. 10. The exchange constant A and K_1 are related to each other. Höfer[8] estimated the exchange constant A to be smaller than $1{,}3\ 10^{-10}$ J/m or smaller than $7{,}8\ 10^{-11}$ J/m, depending on the expression derived by the theory of micromagnetism. In this paper we used for $A = 1{,}3\ 10^{-10}$ J. One still has to add the expansion parameter $\lambda = 0.00297$ formally introduced, which is indeed a small parameter for nickel.

To control the regular alignment of the Bloch walls we used the Bitter pattern technique and applied external magnetic fields between 2 and 7 mT (see Fig. 6). For smaller or higher magnetic fields, these structures become indistinct and disappear completely for the saturation magnetization of about 30 mT. The optimal range can be studied even more precisely by neutron scattering. In Table I the results of the calculation of the boundary condition problem are given. From these calculations one obtains the constant angle θ_0 in the domains.

The energy contained in the Bloch wall per unit surface and the Bloch wall thickness W_L can be calculated from the lowest order of the expansion in λ [see Eqs. (3) and (4)]—corresponding to the method described by Hubert[11] —or up to the first order in λ as given by Eq. (5) (see Table II). This means that with an increasing external magnetic field the angle θ_0 between the magnetization vector and the crystal axis decreases and in the same way the energy necessary for the rotation and the Bloch wall thickness decreases.

TABLE I. The calculated angle θ_0 in the domains for different values of the external magnetic field H_a.

H_a [A/m]	I [mT]	θ_0
796	1	33,3°
1592	2	31,5°
2397	3	29,7°
3183	4	27,9°
3979	5	26,2°
4775	6	24,4°
5570	7	22,5°

TABLE II. The energy per surface unit and the Bloch wall thickness in dependence on the external magnetic field in zero and first order of the expansion in λ.

I [mT]	E_0/ε_0	W_L^0 [nm]	E_1/ε_0	W_L^1 [nm]
1	1,179	460,8	1,195	453,7
2	1,125	449,1	1,111	442,1
3	1,038	439,8	1,024	431,3
4	0,949	431,3	0,935	421,1
5	0,829	424,4	0,843	411,3
6	0,765	416,5	0,749	401,5
7	0,671	409,9	0,655	391,5

To verify these theoretical predictions an extensive series of measurements have been performed to determine with high accuracy the intensity of refracted and unrefracted neutrons for various glancing angles α. The intensity ratio of the refracted and the unrefracted beams is proportional to the Bloch wall thickness W_L. For a given external magnetic field we obtained a series of data in dependence of the glancing angle α and observed a certain dependence of refracted neutrons on the external magnetic field strength (see Fig. 7): the larger the external field, the smaller is the intensity of the refracted neutrons.

To go more into the details we show a set of curves for different external magnetic fields in Figs. 4, 8(a), and 8(b).

The theoretical curves were calculated with the quantum-mechanical Ansatz.[15] For the passage of unpolarized neutrons through a Bloch wall, we used the treatment given in Ref. 8 [solution of Schrödinger's equation for a neutron spinor in an external magnetic field, see Eq. (8)]. The bends in the curves at $\alpha \sim 90'$ correspond to the passage through two or more Bloch walls. The experimental data are compared with different Bloch wall thicknesses denoted on the right-hand side of the figures.

V. DISCUSSION OF THE RESULTS

In this work we present the first precise calculations and measurements of the Bloch wall thickness of a nickel single

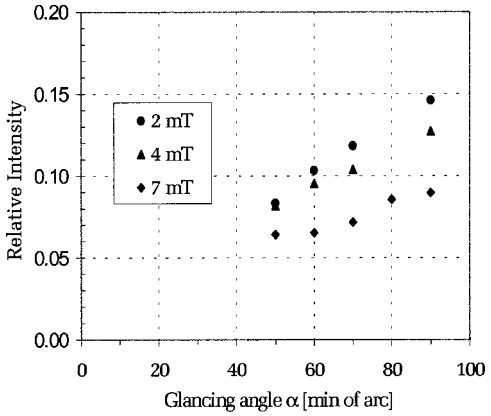

FIG. 7. The intensity of refracted neutrons in dependence of the glancing angle α on different external magnetic fields I [mT].

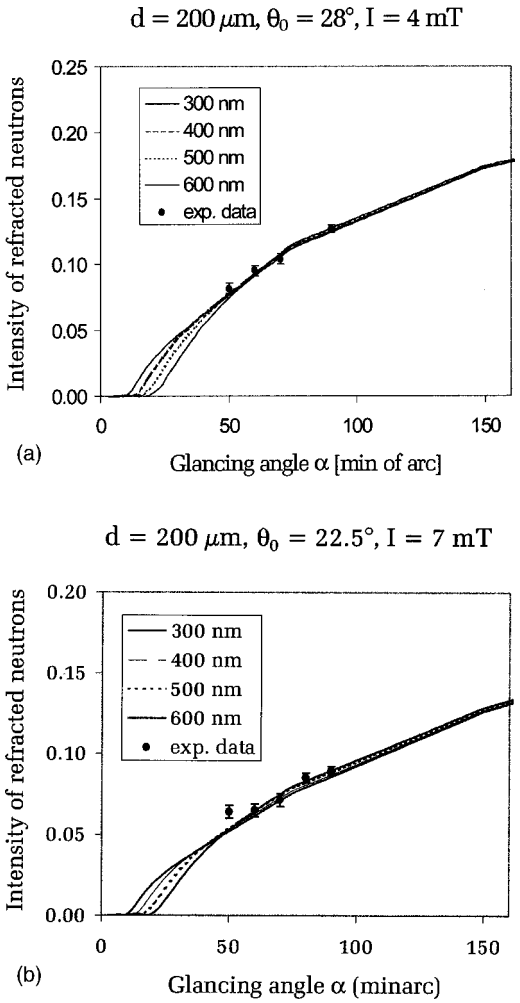

FIG. 8. (a), (b) The normalized intensity of refracted neutrons as a function of the glancing angle α for magnetic fields of 4 and 7 mT with the corresponding domain sizes d and angles θ_0.

crystal for given experimental parameters. The theoretical approach includes external magnetic forces, and the measurements are described in detail. This work sums up the best experimental studies and accomplishes a series of measurements started in Ref. 16. The quantum mechanic description of the interaction of neutrons with Bloch walls agrees well with the predictions of the Bloch wall thickness obtained by the theory of micromagnetism. The experimental points confirm the QM treatment within the experimental error bars. The experimental data follow the theoretical functions even in the case of the passage through two or more Bloch walls. Up to now these results are the most reliable data for Bloch walls in bulk nickel crystals.

Nevertheless we have to mention the experimental difficulties involved in the measurement of refracted neutrons at glancing angles α less than $90'$ (where different Bloch wall thickness can be distinguished). However, the precision of the experimental data is sufficient for an improved and very reliable determination of the Bloch wall thickness: W_L is of the order of some hundreds of nanometers which is in agreement with former published values.[16]

There are other restrictions which should be overcome to yield a much better accurate value of W_L. They all are related to the fact, that the intensity of the refracted neutrons depends not only on the Bloch wall thickness, but also on other parameters which cannot yet be sufficiently controlled. One parameter is the domain size d. It is very difficult to exactly reproduce this domain size after a readjustment of the double crystal diffractometer. The measurements presented in this paper were obtained within nearly two years, taking up several reactor cycles. Due to the broad state of minimum energy the domain size d is not necessarily always the same, even if one applies the same external magnetic field.[17] Another parameter is the value of the constant A which up to now is not accurate enough, and the angle θ_0, which strongly determines the absolute height and slope of the calculated curves. It is related to the boundary condition problem and corresponds to a minimum of the free energy. As far as micromagnetism is a reliable model, there is no reason why this value should not be a stable solution. Finally, the nickel sample we used for all investigations is misoriented by approximately 15° against the crystal axis, e.g., the Bloch walls are not parallel to the crystal surface. From the theoretical point of view one should include this effect into the calculation, generalizing it for a two-dimensional wall. But such a generalization is a very complex project. As the condition $G(\theta_0,\phi_a)=G(\theta_0,\phi_e)\equiv G_\infty$ is no longer fulfilled, the Bloch walls can move. This was checked but we never observed such a motion experimentally. However, such an extreme slow motion cannot be so far fully ruled out. The presented theory together with these series of experiments show, to date, the best agreement of experimental results with the theoretical predictions obtained from the theory of micromagnetism.

ACKNOWLEDGMENTS

This work was supported by the BMBF Project No. 03-TR5TFH and by the TFH-Hypatia Program. The authors wish to thank Misera and Schäfer for fruitful discussions, suggestions and for the help studying the surface of the crystal.

[1] W. Heisenberg, Z. Phys. **49**, 619 (1928); L. Landau and E. Lifshitz, Phys. Z. Sowjetunion **8**, 153 (1935); E. Lifschitz, J. Phys. (France) **8**, 337 (1944).
[2] L. Néel, Colloq. Phys. **25**, 1 (1944).
[3] B. A. Lilley, J. Theor. Exp. Appl. Phys. **41**, 792 (1950).
[4] Ch. Schwink and H. G. Spreen, Phys. Status Solidi **10**, 57 (1965).
[5] H. Strothmann and O. Schärpf, J. Magn. Magn. Mater. **9**, 257 (1978); O. Schärpf and K. Brandt, *ibid.* **9**, 252 (1978); A. Höfer, H. Strothmann, and W. Treimer, Physica B **234–236**, 582 (1997); A. Höfer and W. Treimer, *ibid.* **241–243**, 1231 (1998).

[6] O. Schärpf, R. Seifert, and H. Strothmann, J. Magn. Magn. Mater. **13**, 293 (1979); O. Schärpf, A. Bierfreund, and H. Strothmann, *ibid.* **13**, 243 (1979).
[7] A. Hubert and R. Schäfer, *Magnetic Domains* (Springer-Verlag, Berlin, 1998).
[8] A. Höfer, Ph.D. thesis, Technische Universität Berlin, 1998.
[9] W. F. Brown, Jr., *Micromagnetics* (Krieger, Huntington, NY, 1978).
[10] H. Kronmüller and A. Seeger, in *Moderne Probleme der Metallphysik*, edited by A. Seeger (Springer-Verlag, Berlin, 1966), Vol. 2.
[11] A. Hubert, *Theorie der Domänenwände in geordneten Medien* (Springer-Verlag, Berlin, 1974).
[12] W. Döring, Z. Naturforsch. A **3**, 373 (1948).
[13] Landolt-Börnstein, Numerical Data and Functional Relationships in Science and Technology, edited by K.-H. Hellwege and A. H. Hellwege, New Series, Group III, Vol. 19a (Springer-Verlag, Berlin, 1986).
[14] U. Keyser, Ph.D. thesis, Technische Universität Braunschweig, 1977.
[15] O. Schärpf, Habilitationsschrift, TU Braunschweig, 1976.
[16] W. Treimer, A. Höfer, and H. Strothmann, J. Appl. Crystallogr. **30**, 849 (1997).
[17] R. Schäfer (private communication).